Eur. Phys. J. B **52**, 411–419 (2006)
DOI: 10.1140/epjb/e2006-00315-6

THE EUROPEAN PHYSICAL JOURNAL B

Influence of inter-dot Coulomb repulsion and exchange interactions on conductance through double quantum dot

G. Michałek[a] and B.R. Bułka

Institute of Molecular Physics, Polish Academy of Sciences, ul. Mariana Smoluchowskiego 17, 60–179 Poznań, Poland

Received 28 April 2006
Published online 2 August 2006 –

Abstract. Conductance and other physical quantities are calculated in double quantum dots (DQD) connected in series in the limit of coherent tunnelling using a Green's function technique. The inter-dot Coulomb repulsion and the exchange interaction are studied by means of the Kotliar and Ruckenstein slave-boson mean-field approach. The crossover from the atomic to the molecular limit is analyzed in order to show how the conductance in the model depends on the competition between the level broadening (dot-lead coupling) and the dot-dot transmission. The double Kondo effect was found in the gate voltage characteristics of the conductance in the atomic limit. In the case, when each dot accommodates one electron, the Kondo resonant states are formed between dots and their adjacent leads and transport is dominated by hopping between these two resonances. In the molecular limit the conductance vanishes for sufficiently low gate voltages, which means the Kondo effect disappeared. For small dot-lead coupling the transport characteristics are very sensitive on the influence of the inter-dot Coulomb repulsion and the position of the local energy level. The resonance region is widened with increase of the inter-dot Coulomb interactions while the exchange interaction has opposite influence.

PACS. 72.15.Qm Scattering mechanisms and Kondo effect – 73.63.-b Electronic transport in nanoscale materials and structures – 73.63.Kv Quantum dots

1 Introduction

In the last years, due to the spectacular advances in modern photolithography and self-assembly techniques, electron transport through few-electron quantum dots has been the subject of many experimental and theoretical studies [1,2]. Especially, the double quantum dot (DQD) systems in both parallel and serial configurations have attracted a lot of interest. The small size and low power dissipation have stimulated a number of proposals for their use in spintronic devices and as qubits for future quantum computers [3,4]. In addition, transport studies in DQD allow one to investigate many physical problems like singlet-triplet transitions, Pauli spin blockade and competition between the Kondo effect and the antiferromagnetic correlations between spins of the DQD. There are many papers treating transport through DQD using different models and techniques of calculations like numerical renormalization group (NRG) [5,6], equation of motion (EOM) [7] and slave-bosons (SB) [8–10]. Many of the models take into account on-site Coulomb interactions U only (e.g. [11–13]). However, it was shown recently, that the exchange interaction J can significantly influence Kondo effect near singlet-triplet transition in multilevel quantum dot [14]. In DQD system apart from exchange interactions between electrons located on the same dot appears also inter-site effective exchange $J_{eff} \approx 4t_{12}^2/U$ [8,15]. J_{eff} interactions are antiferromagnetic and usually are small in the case of large on-site Coulomb repulsion U and small dot-dot coupling t_{12} [14]. Very often these small interactions are omitted, but it was pointed out by Aono and Eto [8], that even small antiferromagnetic J_{eff} can significantly change behavior of the conductance and compete with the Kondo effect [5,8,9]. Unfortunately it was reported, that the slave-boson techniques cannot treat an effective exchange J_{eff} processes properly [5]. However, one can introduce in DQD additional exchange interaction J between spins localized on both dots. This allows to study how both: anti- and ferromagnetic orders influence the Kondo effect in the DQD system in the slave-boson approach.

The important parameter in DQD systems is the inter-dot Coulomb interaction U_{12}, which is determined by the mutual dot-dot capacitance (e.g. [16]). This interaction determines an energy, which one has to pay in order to add second electron to the DQD system. An interesting question is how this interaction together with exchange affect transport through the DQD connected in series?

The effect of finite U_{12} and J on transport properties of double quantum dots has been reported previously by Apel et al. [17] in the case when the two dots are inserted into the leads. Results have been obtained by an exact diagonalization of a cluster composed by the double-dot and its vicinity. However, the authors present only the results for weakly coupled dots (when dot-lead coupling is

[a] e-mail: grzechal@ifmpan.poznan.pl

much larger than dot-dot hopping) and did not discuss in details the nature of the effect.

Very useful tools for description of strongly correlated electron systems (large on-site Coulomb repulsion), in particular small QD, are slave-boson mean-field approaches (SBMFA). The main idea of the SBMFA is the transformation of the strongly correlated Hamiltonian to an effective non-interacting one by introduction of auxiliary Bose fields. There are two main slave-boson schemes in the literature, which can be adjusted to describe electron transport through quantum dots system: Coleman [18] and Kotliar-Ruckenstein [19] formulations. Coleman slave-boson formulation is restricted to the infinite intra-dot Coulomb repulsion U, while Kotliar-Ruckenstein scheme can be used for arbitrary U (from $U = 0$ up to $U = \infty$). Both approaches can be applied for low temperatures [18,20] and give correct results for spin fluctuations in the Kondo regime [12,20–22]. Since charge fluctuations are not included at the mean-field approximation [12] applicability of these approaches in studying non-linear transport is restricted to the limit of small source-drain voltages [23]. Important effects of correlations and formation of many-particle states are also outside the scope of SB in the form proposed by Coleman and Kotliar-Ruckenstein.

In [23] Dong and Lei compare results obtained for Coleman and Kotliar-Ruckenstein slave-boson formulations. Authors found that KR slave-bosons are more precise theoretical tool than Coleman formulation. At $T = 0$ the KR SBMFA is equivalent to the results obtained from the analytical technique: Gutzwiller variational wave function. Moreover KR SBMF scheme provides a good tool for investigating linear transport through QD over a very wide range of the energy including both Kondo and non-Kondo regimes (e.g. mixed-valence). The advantage of the method is, that can be very easy extended to the more complicated systems like e.g.: multilevel quantum dots, hybrid mesoscopic devices or Aharonov-Bohm rings [23]. Within generalization of this approach one can also study Kondo effect in external magnetic field, non-equilibrium situations and finite temperature [14,23,24].

In a paper we extend the Kotliar-Ruckenstein slave-boson mean-field approach to calculate conductance and other transport properties of the system consisting of DQD coupled in series for various coupling strength. Our generalization is similar to that proposed by Dong and Lei to study singlet-triplet Kondo effect in multilevel quantum dots [14]. In order to analyze the role of the inter-dot Coulomb repulsion as well as the role of anti- and ferromagnetic interactions on the conductance we have introduced the slave-boson operators not only for single-particle levels but also for many-body states: singlet and triplet.

The paper is organized as follows: in Section 2 we describe the formalism used for calculation of the conductance and other characteristics of the system. The results of our numerical computations are presented in Section 3. First we will analyze in detail the role of the various coupling strength on transport properties through DQD in three different situation: (a) the Kondo regime, when the dot level energy is much below the Fermi energy; (b) the mixed valence regime, when the single electronic level is close to the Fermi energy; and (c) the empty orbital regime, when the energy levels of the dot lie above Fermi energy in the leads. In this part we will also present how the inter-dot Coulomb repulsion influence transport properties of the system. Next we will study how the conductance and other transport properties changes if we continuously sweep energy of the QD levels (which can be done e.g. by change of the gate voltage). In the case, when the inter-dot coupling is weaker than the dot-lead coupling, each dot accommodates one electron and forms the Kondo resonant state with conducting electrons in a lead. In the opposite limits, when the inter-dot coupling exceeds level broadening, the conductance vanishes for sufficiently low gate voltages, which means the Kondo effect disappeared. In the last part of the Section 3 we will analyze the role of the anti- and ferromagnetic inter-dot exchange interactions. We will show how these interactions influence the conductance and the Kondo effect. We will also study the competition between ferromagnetic interactions as well as Coulomb repulsion and coupling strength. In Section 4 final remarks are given.

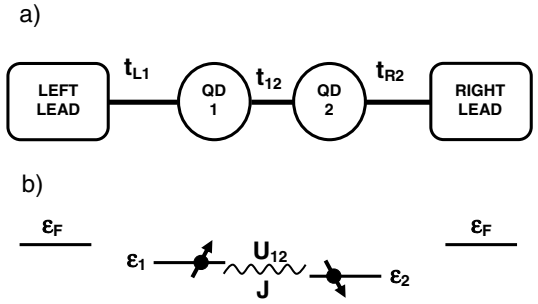

Fig. 1. (a) Schematic view of the serially coupled quantum dots. The dots are coupled via tunnel hopping t_{12}. They are connected only to its adjacent electrodes via t_{L1} and t_{R2}. (b) Schematic electronic structure of the system. Each dot has only one single electronic level ε_j, $j = 1, 2$. U_{12} and J denotes Coulomb repulsion and exchange interactions, respectively.

2 Description of the model

We consider a system, which is composed of two small quantum dots connected in series with electrodes (Fig. 1a). The Hamiltonian for the system is:

$$H = \sum_{j,\sigma} \epsilon_j c^\dagger_{j\sigma} c_{j\sigma} + t_{12} \sum_{\sigma} \left(c^\dagger_{1\sigma} c_{2\sigma} + c^\dagger_{2\sigma} c_{1\sigma} \right) + \sum_{\alpha,j,k,\sigma} t_{\alpha j} \left(c^\dagger_{\alpha k\sigma} c_{j\sigma} + c^\dagger_{j\sigma} c_{\alpha k\sigma} \right) + \sum_{j,\sigma} U_j \hat{n}_{j\sigma} \hat{n}_{j\bar{\sigma}} + U_{12} \sum_{\sigma,\sigma'} \hat{n}_{1\sigma} \hat{n}_{2\sigma'} - J \boldsymbol{S}_1 \cdot \boldsymbol{S}_2 + \sum_{\alpha,k,\sigma} \epsilon_{\alpha k} c^\dagger_{\alpha k\sigma} c_{\alpha k\sigma}. \quad (1)$$

The first term corresponds to electrons on quantum dots ($j = 1, 2$) with electronic level ϵ_j, where $c^\dagger_{j\sigma}$ and $c_{j\sigma}$ are

creation and annihilation operators for an electron of spin projection $\sigma =\uparrow,\downarrow$ on dot $j = 1, 2$. Hopping between the dots (t_{12}) and coupling to the leads ($t_{\alpha j}$) are delineated by the second and the third parts, respectively. The matrix elements $t_{\alpha j}$ are assumed to be independent of spin and energy. The on-site Coulomb interactions U_j and Coulomb repulsion U_{12} between electrons localized on different dots are described by the next two term respectively, where a number operator $\hat{n}_{j\sigma} = c^{\dagger}_{j\sigma}c_{j\sigma}$. And finally

$$-J\boldsymbol{S}_1\cdot\boldsymbol{S}_2 = -J\sum_{\sigma}\left(\hat{n}_{1\sigma}\hat{n}_{2\sigma}-\hat{n}_{1\sigma}\hat{n}_{2\bar{\sigma}}+2c^{+}_{1\sigma}c_{1\bar{\sigma}}c^{+}_{2\bar{\sigma}}c_{2\sigma}\right) \quad (2)$$

corresponds to ferromagnetic ($J > 0$) or antiferromagnetic ($J < 0$) interactions between magnetic moments of electrons localized on the first and the second QD. The last part of equation (1) characterizes noninteracting electrons in the leads, labelled by $\alpha = L, R$, where $c^{\dagger}_{\alpha k\sigma}$ ($c_{\alpha k\sigma}$) is the creation (annihilation) operator for electron with momentum k in the electrode α, $\epsilon_{\alpha k}$ denotes the electron energy.

A linear transport through the system can be studied by means of the Kotliar and Ruckenstein (KR) slave-boson mean-field (SBMF) scheme [19]. In this method the strongly correlated Hamiltonian (Eq. (1)) is transformed to an effective, noninteracting one, through introduction of auxiliary boson operators. A disadvantage of the SBMF approach is that does not take into account many-electronic levels like e.g. singlet or triplet. In order to take these states into consideration we have modified SBMF approach and introduced slave-boson operators not only for single-particle levels but also for singlet and triplet states. We also take into account strong Coulomb interactions on each dot ($U_1 = U_2 = \infty$) and restrict ourselves to the lowest energy level, in which each dot can be occupied only by one electron with spin $\sigma =\uparrow$ or $\sigma =\downarrow$, respectively. According to the SBMF, in addition to the electron creation (annihilation) operators $f^{\dagger}_{j\sigma}$ ($f_{j\sigma}$), we introduce a set of auxiliary boson operators $e^{\dagger}$ (e), $p^{\dagger}_{j\sigma}$ ($p_{j\sigma}$), $d^{\dagger}_{1S_Z}$ (d_{1S_Z}) and $d^{\dagger}_0$ (d_0), which act, respectively, as projectors onto the empty ($|0,0\rangle$), singly occupied ($|\sigma,0\rangle$, $|0,\sigma\rangle$), triplet ($|\sigma,\sigma\rangle$, $(|\uparrow,\downarrow\rangle+|\downarrow,\uparrow\rangle)/\sqrt{2}$) and singlet ($(|\uparrow,\downarrow\rangle-|\downarrow,\uparrow\rangle)/\sqrt{2}$) electron states. In order to eliminate unphysical states these operators must satisfy the completeness relations for the slave-boson operators

$$I \equiv e^{\dagger}e+\sum_{j\sigma}p^{\dagger}_{j\sigma}p_{j\sigma}+\sum_{S_Z=\bar{1},0,1}d^{\dagger}_{1S_Z}d_{1S_Z}+d^{\dagger}_0d_0 = 1 \quad (3)$$

and the charge conservation

$$Q_{j\sigma} \equiv c^{\dagger}_{j\sigma}c_{j\sigma} = p^{\dagger}_{j\sigma}p_{j\sigma}+\sum_{S_Z=\bar{1},1}d^{\dagger}_{1S_Z}d_{1S_Z}+\frac{1}{2}\left(d^{\dagger}_{10}d_{10}+d^{\dagger}_0d_0\right). \quad (4)$$

These constraints have been incorporated with the Lagrange multipliers λ and $\lambda_{j\sigma}$ into the effective Hamiltonian

$$\begin{aligned}H_{eff} = &\sum_{\alpha,k,\sigma}\epsilon_{\alpha k}c^{\dagger}_{\alpha k\sigma}c_{\alpha k\sigma}+\sum_{j,\sigma}\epsilon_j f^{\dagger}_{j\sigma}f_{j\sigma}\\ &+t_{12}\sum_{\sigma}\left(z^{\dagger}_{1\sigma}f^{\dagger}_{1\sigma}f_{2\sigma}z_{2\sigma}+z^{\dagger}_{2\sigma}f^{\dagger}_{2\sigma}f_{1\sigma}z_{1\sigma}\right)\\ &+\sum_{\alpha,j,k,\sigma}t_{\alpha j}\left(c^{\dagger}_{\alpha k\sigma}f_{j\sigma}z_{j\sigma}+z^{\dagger}_{j\sigma}f^{\dagger}_{j\sigma}c_{\alpha k\sigma}\right)\\ &+(U_{12}-J)\sum_{S_Z=\bar{1},0,1}d^{\dagger}_{1S_Z}d_{1S_Z}+(U_{12}+3J)d^{\dagger}_0d_0\\ &+\lambda(I-1)+\sum_{j\sigma}\lambda_{j\sigma}\left(f^{\dagger}_{j\sigma}f_{j\sigma}-Q_{j\sigma}\right) \quad (5)\end{aligned}$$

where the QD fermion operators $c^{\dagger}_{j\sigma}$ ($c_{j\sigma}$) in the hopping term of equation (1) are replaced by the operator $z^{\dagger}_{j\sigma}f^{\dagger}_{j\sigma}$ ($f_{j\sigma}z_{j\sigma}$), where

$$z_{j\sigma} = \frac{e^{\dagger}p_{j\sigma}+p^{\dagger}_{j\sigma}d_{1S_z}+\frac{1}{2}p^{\dagger}_{j\bar{\sigma}}(d_{10}+d_0)}{\sqrt{Q_{j\sigma}}\sqrt{1-Q_{j\sigma}}}, \quad (6)$$

where for $\sigma =\uparrow$ ($\downarrow$) one take $S_z = 1(\bar{1})$.

From the effective Hamiltonian (Eq. (5)) one can derive (using the saddle-point approximation) a set of self-consistent equations for the slave-boson operators. We use the mean-field approximation, in which all slave boson operators in these equations and in the constraints are treated as c-numbers and replaced by their expectation values. The Zeeman splitting is also neglected, so that $p_{j\sigma} = p_j$, $d_{1S_z} = d_1$ and $z_{j\sigma} = z_j$. We obtained:

$$\begin{aligned}e^2+2p_1^2+2p_2^2+3d_1^2+d_0^2 &= 1,\\ n_1 = 2p_1^2+3d_1^2+d_0^2 &= \sum_{\sigma}\int\frac{d\omega}{2\pi i}G^{<}_{1\sigma,1\sigma}(\omega),\\ n_2 = 2p_2^2+3d_1^2+d_0^2 &= \sum_{\sigma}\int\frac{d\omega}{2\pi i}G^{<}_{2\sigma,2\sigma}(\omega),\\ x_{12}\left(\frac{\partial\ln z_1}{\partial e}+\frac{\partial\ln z_2}{\partial e}\right)&\\ +x_{L1}\frac{\partial\ln z_1}{\partial e}+x_{R2}\frac{\partial\ln z_2}{\partial e}+2\lambda e &= 0,\\ x_{12}\left(\frac{\partial\ln z_1}{\partial p_1}+\frac{\partial\ln z_2}{\partial p_1}\right)+x_{L1}\frac{\partial\ln z_1}{\partial p_1}&\\ +x_{R2}\frac{\partial\ln z_2}{\partial p_1}+4(\lambda-\lambda_1)p_1 &= 0,\\ x_{12}\left(\frac{\partial\ln z_1}{\partial p_2}+\frac{\partial\ln z_2}{\partial p_2}\right)+x_{L1}\frac{\partial\ln z_1}{\partial p_2}&\\ +x_{R2}\frac{\partial\ln z_2}{\partial p_2}+4(\lambda-\lambda_2)p_2 &= 0,\\ x_{12}\left(\frac{\partial\ln z_1}{\partial d_1}+\frac{\partial\ln z_2}{\partial d_1}\right)+x_{L1}\frac{\partial\ln z_1}{\partial d_1}&\\ +x_{R2}\frac{\partial\ln z_2}{\partial d_1}+6(\varepsilon_T+\lambda-\lambda_1-\lambda_2)d_1 &= 0,\\ x_{12}\left(\frac{\partial\ln z_1}{\partial d_0}+\frac{\partial\ln z_2}{\partial d_0}\right)+x_{L1}\frac{\partial\ln z_1}{\partial d_0}&\\ +x_{R2}\frac{\partial\ln z_2}{\partial d_0}+2(\varepsilon_S+\lambda-\lambda_1-\lambda_2)d_0 &= 0, \quad (7)\end{aligned}$$

where

$$x_{12} = \frac{\tilde{t}_{12}}{\pi} \sum_{\sigma} \int d\omega \mathrm{Im}\left[G^{<}_{1\sigma,2\sigma}(\omega)\right],$$
$$x_{L1} = \frac{\tilde{t}_{L1}}{\pi} \sum_{\sigma} \int d\omega \mathrm{Im}\left[G^{<}_{L\sigma,1\sigma}(\omega)\right],$$
$$x_{R2} = \frac{\tilde{t}_{R2}}{\pi} \sum_{\sigma} \int d\omega \mathrm{Im}\left[G^{<}_{R\sigma,2\sigma}(\omega)\right], \quad (8)$$

$\tilde{t}_{L1} = t_{L1} z_1$, $\tilde{t}_{R2} = t_{R2} z_2$ and $\tilde{t}_{12} = t_{12} z_1 z_2$.

The current flowing through the system is calculated from the time evolution of the occupation number $N_L = \sum_{k,\sigma} c^{\dagger}_{\alpha k\sigma} c_{\alpha k\sigma}$ for electrons in the left electrode

$$\mathcal{J} \equiv -e\left\langle \dot{N}_L \right\rangle = \frac{-ie}{\hbar}\left\langle \left[H_{eff}, \sum_{k,\sigma} c^{\dagger}_{Lk\sigma} c_{Lk\sigma} \right] \right\rangle$$
$$= \frac{2e}{\hbar} \tilde{t}_{L1} \sum_{\sigma} \int d\omega Re\left[G^{<}_{1\sigma,L\sigma}(\omega)\right]. \quad (9)$$

The appropriate Green functions (seen in Eqs. (7–9)) are calculated with the help of the Langreth analytical continuation rules [25] and have rather complicated form, e.g.

$$G^{<}_{1\sigma,L\sigma}(\omega) = \frac{2\tilde{\Gamma}_L}{\tilde{t}_{L1}} \left\{ \frac{\left[(\omega - \tilde{\epsilon}_2)\, i - \tilde{\Gamma}_R\right] f_L(\omega)}{(\omega - \tilde{\epsilon}_{r-})(\omega - \tilde{\epsilon}_{r+})} \right.$$
$$\left. - \frac{\tilde{\Gamma}_L\left[(\omega - \tilde{\epsilon}_2)^2 + \tilde{\Gamma}_R^2\right] f_L(\omega) + \tilde{\Gamma}_R \tilde{t}_{12}^2 f_R(\omega)}{(\omega - \tilde{\epsilon}_{r-})(\omega - \tilde{\epsilon}_{r+})(\omega - \tilde{\epsilon}_{a-})(\omega - \tilde{\epsilon}_{a+})} \right\} \quad (10)$$

where

$$\tilde{\epsilon}_{r(a)\mp} = \frac{\tilde{\epsilon}_1 + \tilde{\epsilon}_2 + i\xi(\tilde{\Gamma}_L + \tilde{\Gamma}_R)}{2}$$
$$\mp \frac{\sqrt{[\tilde{\epsilon}_1 - \tilde{\epsilon}_2 + i\xi(\tilde{\Gamma}_L - \tilde{\Gamma}_R)]^2 + 4\tilde{t}_{12}^2}}{2}, \quad (11)$$

$\xi = -1$ for $\tilde{\epsilon}_{r\mp}$ ($\xi = 1$ for $\tilde{\epsilon}_{a\mp}$), $\tilde{\epsilon}_j = \epsilon_j + \lambda_j$, $\tilde{\Gamma}_L = \Gamma_L z_1^2$ ($\tilde{\Gamma}_R = \Gamma_R z_2^2$), $\Gamma_L = \pi\rho_L t_{L1}^2$ ($\Gamma_R = \pi\rho_R t_{R2}^2$). $f_\alpha(\omega)$ denotes Fermi-Dirac distribution function in the electrode α with a chemical potential μ_α shifted by $\pm eV/2$ for $\alpha = L, R$ respectively, V is an applied bias voltage and ρ_α is the constant density of states in the electrode $\alpha = L, R$.

Finally, in the linear limit, the conductance can be calculated from the formula $G_0 = (\partial\mathcal{J}/\partial V)|_{V=0}$.

3 Results

In this section we will present some results of our numerical computations. The calculations were performed for a symmetrical system. It is assumed that both dots are identical (so $\varepsilon_1 = \varepsilon_2 = \varepsilon_0$) and coupled to its adjacent leads with the same strength $\Gamma = \Gamma_L = \Gamma_R$. The dot-dot coupling t_{12} is chosen as the energy unit. The temperature T and Fermi energy of the leads ε_F are set to be 0.

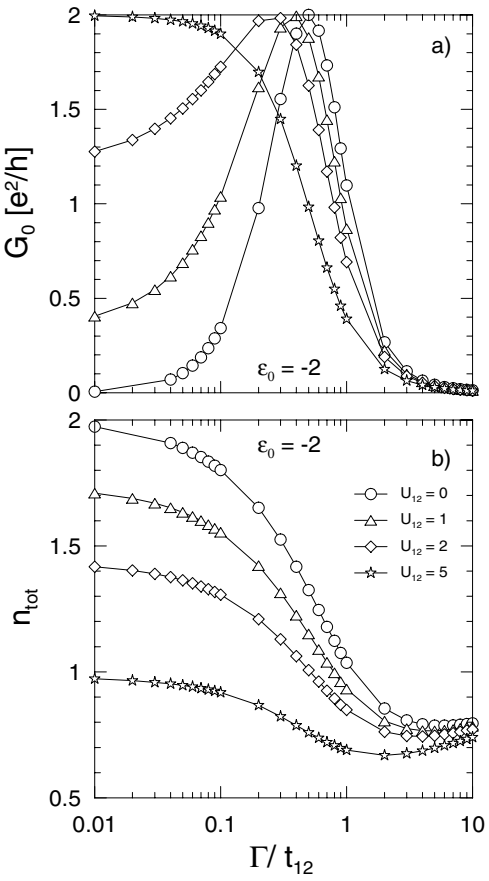

Fig. 2. Conductance G_0 and the total number of electrons n_{tot} as a function of dot-lead coupling Γ.

3.1 Crossover from the two separated dots to the quantum dots dimer

Transport through DQD system strongly depend on competition between the dot-dot and the dot-lead couplings. When the hopping between the quantum dots is much weaker than dot-lead tunnelling one can neglect hybridization (caused by t_{12}) between the dots. Electrons tend to occupy local (individual dot) states so the both dots can be considered separately. By analogy with the isolated atom we will call this regime atomic. In the opposite limit, when the dot-dot binding dominate over dot-lead coupling ($t_{12} \gg t_{\alpha j}$) one can treat DQD as an artificial molecule (dimer). In this molecular regime, the electrons occupy a bonding and anti-bonding orbitals rather than local states. The purpose of this paragraph is to study the crossover from the atomic to the molecular limit, which can be controlled by a change of the level broadening Γ versus dot-dot coupling t_{12}.

The influence of the transition from the atomic to the molecular regime on the conductance is shown in Figure 2a where the conductance G_0 as a function of the tunnel coupling Γ is plotted for several values of inter-dot Coulomb interactions $U_{12} = 0, 1, 2, 5$, in the Kondo regime ($\varepsilon_0 < \varepsilon_F$). The results are obtained on condition that the single electronic level is fixed at $\varepsilon_0 = -2$ below the Fermi energy $\varepsilon_F = 0$. In the absence (and for very weak)

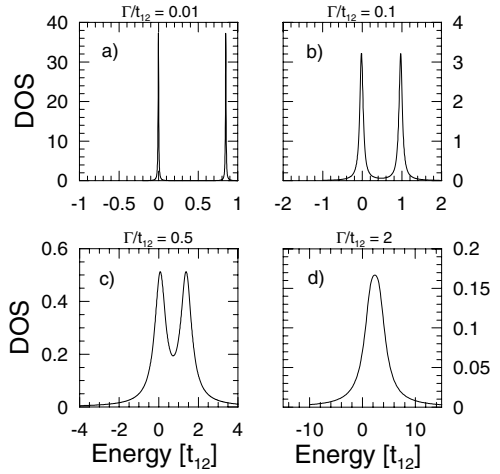

Fig. 3. Density of states for $\varepsilon_0 = -2$, $U_{12} = 2$ and several values of Γ/t_{12}: (a) $\Gamma/t_{12} = 0.01$; (b) $\Gamma/t_{12} = 0.1$; (c) $\Gamma/t_{12} = 0.5$; and (d) $\Gamma/t_{12} = 2$.

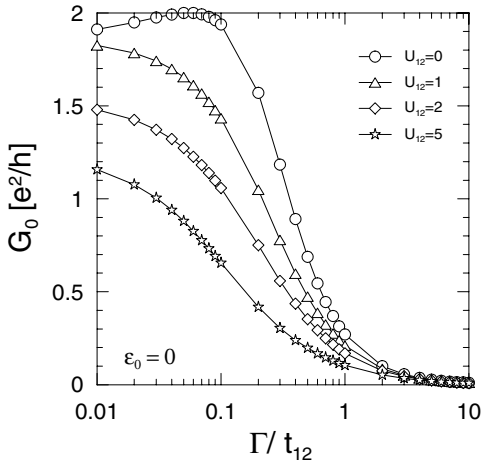

Fig. 4. Conductance as a function of dot-lead coupling Γ in the mixed-valence regime ($\varepsilon_0 = 0$) The parameters are the same as those in Figure 2.

inter-dot interactions U_{12} conductance has a narrow peak (approximately symmetric) with height $2e^2/h$. For larger U_{12}, in the molecular limit ($\Gamma/t_{12} \ll 1$), peaks become asymmetrical because a shoulder arises in the conductance characteristics. The maximum of the peak is shifted with increasing U_{12} to lower value of Γ/t_{12}. The width of the peak also increases. For large U_{12} ($U_{12} > 4t_{12}$) the peak structure disappears and the conductance smoothly increases with decreasing Γ/t_{12}.

The average total occupancy of the DQD is shown in Figure 2b. The characteristics are non-monotonic functions of the parameter Γ/t_{12}. In general the amplitude of n_{tot} decreases with increasing U_{12} while the shape of the curves is similar. One can see that for a sufficiently large U_{12} ($U_{12} > 4t_{12}$) the total number of electrons is always below 1 in whole range of Γ/t_{12}. It suggests that sufficiently large U_{12} make double occupation of the system impossible.

In the molecular limit ($\Gamma/t_{12} \ll 1$, small dot-lead couplings) the conductance and average number of electrons are very sensitive to an increase of the Coulomb interactions U_{12} (see Fig. 2). For $U_{12} = 0$, when the average occupancy of DQD reaches 2, the conductance vanishes as is clearly seen in Figure 2a. On the other hand, for sufficiently large U_{12} ($U_{12} > 4t_{12}$), conductance reaches its maximal value $2e^2/h$ even for very small dot-lead coupling (Fig. 2a).

The dependencies plotted in Figure 2 can be explained with the help of density of states (DOS). As an example, Figure 3 presents DOS for $U_{12} = 2$ and several values of Γ/t_{12}. Let us analyze first the small dot-lead coupling limit $\Gamma/t_{12} \ll 1$. In that case, one sees two well separate very narrow states, one located on the Fermi level and the second above (Fig. 3a). The tunnelling through the state aligned with the Fermi level is responsible for the finite conductance seen in the molecular limit (in the small Γ regime) in Figure 2a. In absence of U_{12}, the conductance vanishes in the molecular regime because DOS peak does not match the Fermi energy. For $U_{12} \neq 0$ however, energy level ε_0 is pinned to the Fermi energy $\varepsilon_F = 0$. The pinning strength can be related to the width of the peak and increases with increasing U_{12}. We have also plotted DOS for different U_{12} (not shown here) and found, that with increasing U_{12} the maximum of the peak is shifted from the value, which lies below ε_F (for $U_{12} = 0$) to the value, which lies above the Fermi level (for large U_{12}). This shift of the position of the energy level is responsible for the drop of n_{tot} observed in Figure 2b with increasing U_{12}. For small U_{12}, when the level lies below the Fermi level, two electrons are in the DQD system and the transport is blocked. If we increase U_{12}, than the energy level is shifted closer to the Fermi level, the peak width is larger and the tail of the peak crosses the Fermi energy, so conductance increases and one can see shoulder in Figure 2a for $\Gamma/t_{12} \ll 1$. If we increase U_{12} even more, then maximum of the DOS peak crosses the Fermi energy. Now, less than one half of the DOS peak lies below Fermi energy, so n_{tot} is less than one on average. However the conductance is still high, because the tail of the peak matches Fermi energy.

For moderate values of Γ/t_{12} one can see from Figures 3b, 3c, that one of the quasi-bond states is still located close to the Fermi energy, which results in a change of the conductance (see Fig. 2a). It is clearly seen from Figure 3 that the width of the peaks increases with increasing Γ and that for a sufficiently large Γ the two DOS peaks merge together (Fig. 3d).

Let us once again take a look in Figure 2 and focus on the atomic limit (for a large dot-lead coupling $\Gamma/t_{12} \gg 1$). The conductance always vanishes in this regime. The suppression of the conductance for $\Gamma \gg t_{12}$ is simply due to the fact, that the maximum of the DOS peak is shifted far above the Fermi level and large difference between Γ and t_{12} is generating an effective potential barrier, which blocks the electron transfer from one dot to another dot. The average number of electrons saturates and depends on the dot level position only, the Coulomb interactions U_{12} does not have any influence.

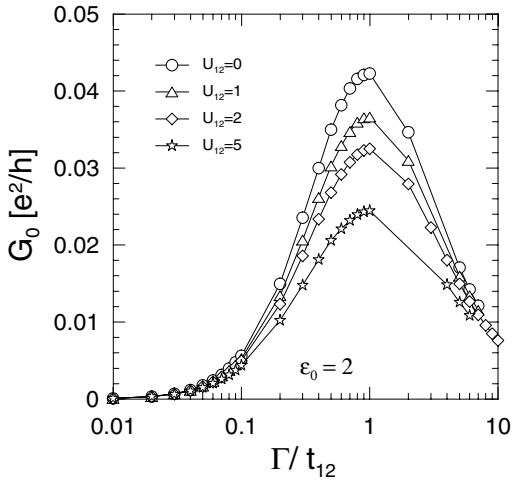

Fig. 5. Conductance as a function of dot-lead coupling Γ in the empty orbital regime ($\varepsilon_0 = 2$). The parameters are the same as those in Figure 2.

In Figure 4, the conductance G_0 in the intermediate valence regime ($\varepsilon_0 = 0$) is plotted. In this regime, in the absence of U_{12} and a small coupling $\Gamma/t_{12} \ll 1$, the system is predominantly in the state with $n_{tot} \geq 1$. The conductance reaches its maximal value $2e^2/h$ only in the absence of U_{12}, when the $n_{tot} \simeq 1$, then decreases. If the Coulomb interactions are present ($U_{12} > 0$) the conductance G_0 monotonically decreases with increasing coupling to the leads. It is clearly seen, that with increasing Coulomb repulsion U_{12} between dots, conductance also decreases. This is because with increasing U_{12} the average occupation (not shown here) of DQD decreases.

Above we have analyzed situations, when electronic level ε_0 lie below or close to the Fermi level, $\varepsilon_0 \leq \varepsilon_F$. Now we will discuss the opposite limit $\varepsilon \gg \varepsilon_F$. It is so called empty orbital regime, because an isolated DQD is empty in the equilibrium. If we turn on coupling to the leads, then the conductance will slowly increase, see Figure 5. In contrast to situation shown in Figure 2, the amplitude of the conductance is two order of magnitude smaller. The maximum of the peaks of G_0 appears when hopping between dots matches dot-lead coupling, $t_{12} = \Gamma$. Further increase of Γ introduces asymmetry between the dot-dot coupling and the level broadening, which leads to worsening of the transport, so the conductance decreases. Contrary to the conductance, which has a small peak, the total number of electrons (n_{tot}) (not shown here) on DQD monotonically increases when the transition of the system from the molecular to the atomic limit occurs.

3.2 Formation of the double Kondo effect in the atomic limit

In the previous section we have studied the crossover from the atomic ($\Gamma \gg t_{12}$) to the molecular ($\Gamma \ll t_{12}$) regime and the influence of this transition on the conductance and other transport characteristics of the system in the Kondo, mixed valence and empty orbital regimes. One sees, that

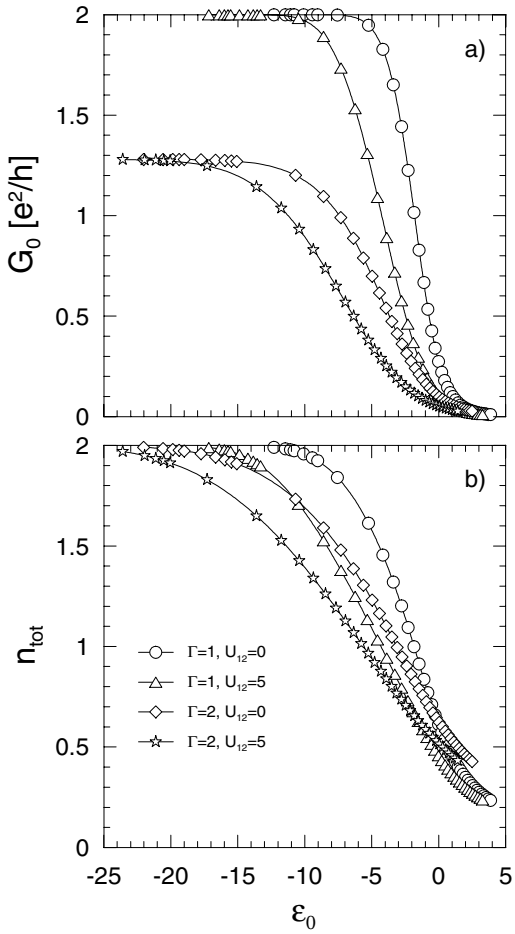

Fig. 6. Conductance (a) and total number of additional electrons in DQD (b) as a function of dot level energy ε_0 for $\Gamma/t_{12} = 1, 2$ and $U_{12} = 0, 5$.

the conductance always vanishes if the system reaches an atomic limit ($\Gamma \gg t_{12}$), see Figures 2, 4 and 5. However, as we will show in this paragraph, when the local electronic level ε_0 lies sufficiently deep below Fermi energy (i.e. $\varepsilon_0 + U_{12} \ll \varepsilon_F$) the finite conductance appears even in the atomic limit. In this very deep Kondo regime each dot accommodates one electron. The local magnetic moment associated with the electron is coupled via an exchange interactions with the conduction electrons in the adjacent lead. So, in this section we will focus our attention on this so called double Kondo effect.

The results of our numerical computations are presented in Figure 6 for several values of U_{12} and $\Gamma/t_{12} = 1, 2$ as a function of the dot level position ε_0. The conductance monotonically increases if the dot level position ε_0 goes below the Fermi level $\varepsilon_F = 0$, (see Fig. 6a). For a very deep position (deep inside the Kondo regime) of the dot level ε_0, there are two additional electrons in the system (Fig. 6b) and the conductance has a plateau (Fig. 6a). Now it will be explained why these plateau appears. Because our system of DQD is symmetric, we deduce from Figure 6b, that there is one electron strongly localized on each QD on average. We have

calculated (it is not shown here) an average value of the local magnetic moment of the dot for $\varepsilon_0 + U_{12} \ll E_F$ and found that is close to the 3/4, which is the value for a free electron. It means that each dot accommodates one electron with spin $\uparrow$ or $\downarrow$ on the energy level laying deep below the Fermi energy. We found that in this regime, close to the Fermi level, arises an effective bonding level $\tilde{\varepsilon}_-$, which is available for the tunnelling processes. The magnetic moment located on the dot is shielded by conduction electrons from the adjacent lead (Kondo singlet state is formed) due to the very big dot-lead coupling. The electron transport through the system is now determined by the hopping between these two Kondo states. Resulting double Kondo effect is clearly seen as an aforementioned wide plateau (Fig. 6a). Conductance approaches its maximal value $G_0 = 2$ for $\Gamma/t_{12} = 1$ and decreases with increasing asymmetry between dot-lead and dot-dot coupling. However even for large asymmetry, the effect is still present (but is weaker). Qualitatively similar results were obtained using a numerical renormalization group method for DQD with a finite on-site repulsion and effective exchange [5,6].

3.3 Resonant transport in the molecular regime

Comparisons of the results, which are presented in Figures 2, 4 and 5, show that in the molecular limit ($\Gamma \ll t_{12}$) the conductance and the average occupation of the dot are very sensitive on the influence of the inter-dot Coulomb repulsion and the position of the local energy level ε_0. In order to understood fully this case the further analysis is needed. So in this section we will investigate the influence of the competition between U_{12} and ε_0 on the transport properties of the system in the molecular regime. For this purpose we have calculated the gate voltage characteristics of the system for several U_{12}. The results of our computations are presented in Figure 7.

In this case the very narrow bonding and anti-bonding states are formed in the double quantum dot. The anti-bonding state $\tilde{\varepsilon}_+$ always lie far above the Fermi energy and does not contribute to the conductance. The bonding level $\tilde{\varepsilon}_-$ crosses the Fermi energy when there is only one additional electron in the DQD dimer. Thus, the resonant tunnelling ($G_0 = 2e^2/h$) only takes place when the effective bonding state $\tilde{\epsilon}_-$ matches the Fermi energy. It can suggests that the conductance peaks are due to the coupling of a magnetic moment of single electron on bonding level with conduction electrons in the leads, i.e. due to the Kondo effect. The peak width increases with increasing coupling ratio. One can clearly see from Figure 7a that for very deep level position conductance vanishes. This decay of conductance is caused by creation of the singlet state by two electrons occupying the bonding orbital. In this case the Kondo resonance does not appear. In Figure 7 it is also shown the influence of inter-dot Coulomb interactions U_{12} on transport through double quantum dot. One can see that the peak is widened and the peak maximum is shifted to deeper gate voltages with increasing inter-dot Coulomb repulsion. This behavior is caused by the increase of the energy of the triplet and singlet states $E_{T,S} \sim 2\epsilon_0 + U_{12}$ with growing Coulomb repulsion U_{12}.

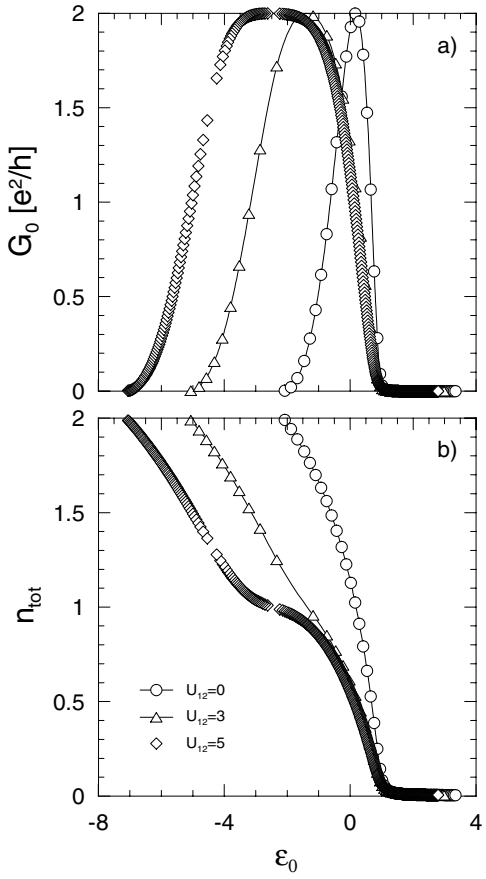

Fig. 7. Conductance (a) and total number of additional electrons in DQD (b) as a function of dot level energy ε_0 for $\Gamma/t_{12} = 0.01$.

3.4 Influence of the exchange interaction

In this section we would like to discuss how the exchange interactions (described by J) influence transport through the system. In particular, we want to investigate in detail how the ferromagnetic as well as antiferromagnetic interaction between electrons located on both dots affect the double Kondo effect. In Figure 8 it is plotted the conductance and the correlation function $\langle \boldsymbol{S}_1 * \boldsymbol{S}_2 \rangle$ as a function of a gate voltage for ferromagnetic ($J > 0$) and antiferromagnetic ($J < 0$) cases in the atomic limit. One can see that with increasing $|J|$ the curves are shifted to the larger value of ε_0 and that width of the transition region (the region, in which conductance increases from zero to its maximal value) is narrowed. So, one can say that the influence of J is opposite to the influence of U_{12} (see Fig. 6). In general the behavior of the conductance does not depend on the sign of J, so anti- and ferromagnetic interactions have the same influence on transport in the model (Fig. 8). The absolute value of the correlation function $\langle \boldsymbol{S}_1 * \boldsymbol{S}_2 \rangle$ grows with decreasing gate voltage. The ferromagnetic interactions ($J > 0$) start to play

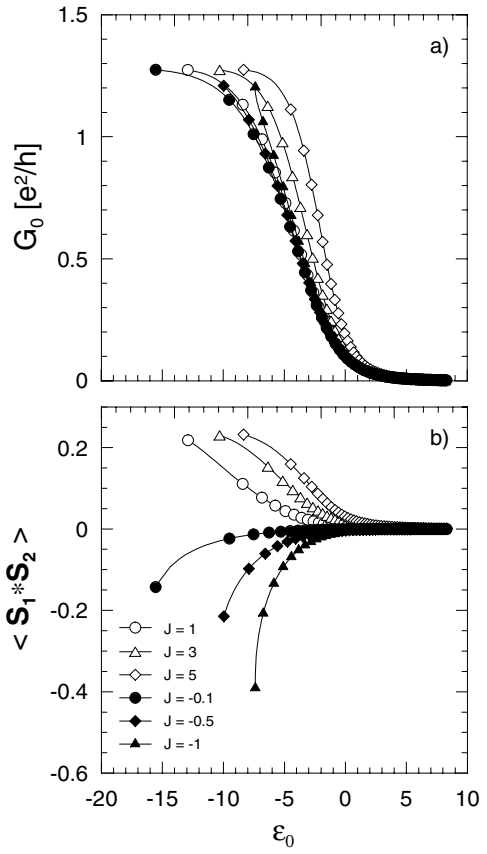

Fig. 8. Conductance (a) and correlation function $\langle \boldsymbol{S}_1 \cdot \boldsymbol{S}_2 \rangle$ (b) as a function of dot level energy ε_0 for $\Gamma/t_{12} = 2$ for several values of J.

a role for larger values of ε_0 than the antiferromagnetic one ($J < 0$), see Figure 8. The amplitude of $\langle \boldsymbol{S}_1 * \boldsymbol{S}_2 \rangle$ for $J > 0$ increases slower than in the antiferromagnetic case. This behavior can be easy explained with the help of the energy of the spin singlet $\varepsilon_S = 2\varepsilon_0 + U_{12} + 3J$ and spin triplet $\varepsilon_T = 2\varepsilon_0 + U_{12} - J$ states. One sees from Figure 8, that in very deep Kondo regime the finite conductance is present even in the case of large anti- and ferromagnetic interactions J between magnetic moments located on the both dots. We have calculated (it is not shown here) that in this regime the total number of additional electrons in the system approaches two, so on each dot one electron is localized. The total magnetic moment of the DQD ($\langle (\boldsymbol{S}_1 + \boldsymbol{S}_2)^2 \rangle = \langle \boldsymbol{S}_1^2 \rangle + \langle \boldsymbol{S}_2^2 \rangle + 2\langle \boldsymbol{S}_1 * \boldsymbol{S}_2 \rangle$) is smaller (larger) than average magnetic moment 3/2 of the two free electrons due to the presence of the antiferromagnetic (ferromagnetic) interaction between the dots. Moreover, for $J > 0$ the total magnetic moment increases monotonically with decrease of the ε_0, while for $J < 0$ it has a local maximum (these results are not shown here). This maximum appears as a result of the competition between square of the local spins $\langle \boldsymbol{S}_j^2 \rangle$ and the correlator $\langle \boldsymbol{S}_1 * \boldsymbol{S}_2 \rangle$. So, we have situation similar to that analyzed in Section 3.2. However in the absence of exchange interaction (see Sect. 3.2), the singlet and the triplet states have the same energy and one cannot distinguish parallel and antiparallel spin configuration. In the presence of exchange interaction the singlet and triplet states have different energy. One can easily find, that for ferromagnetic interaction the parallel configuration of spins on the dots is preferred (Fig. 8b) and in the very deep Kondo regime mainly the spin triplet state with energy $\varepsilon_T = 2\varepsilon_0 + U_{12} - J$ is occupied. In the opposite case, when the interactions are antiferromagnetic, the spin singlet state is formed (Fig. 8b) between the electrons located on the quantum dots. One sees from our calculations that the double Kondo effect survives even for large ferromagnetic ($J = 5$) and antiferromagnetic ($J = -1$) spin-spin correlations.

We have also studied the influence of the exchange interactions on the system in the molecular regime for $\Gamma \ll t_{12}$ (the results of our calculations are not present here). The conductance has a peak, like in Figure 7. The ferromagnetic interaction shifts maximum of the conductance peak to the larger value of ε_0 and the peak width is narrowed. In the double occupancy regime ($n_{tot} = 2$) the conductance vanishes (like in Fig. 7).

The competition between the antiferromagnetic interaction and the Kondo effect has been studied by Aono and Eto in [8]. The authors have calculated conductance in the DQD system using the Coleman slave-boson formalism [18], in which on-site Coulomb interaction is assumed to be $U = \infty$. They introduced to the model an effective (small) antiferromagnetic interactions $J_{eff} \approx 4t_{12}^2/U$ between magnetic moments localized on the both dots. The authors have found that for finite J appears very narrow unitary peak ($2e^2/h$) in the gate voltage dependence of the conductance and that conductance vanishes if ε_0 lie much below Fermi energy. They claim that this behavior is because at sufficiently low gate voltages, a spin-singlet state appears (between magnetic moments localized on both dots) that destroys the Kondo effect (between localized moments and conduction electrons in the lead). We did not find this unitary peak in our calculations, so we do not observe the crossover between double Kondo and spin-singlet state (formed in DQD).

There are two main reasons that this difference can occur. From the one side, similarly to Aono and Eto calculations [8], we have assumed an infinite intra-dot Coulomb repulsion and introduced exchange interaction as a parameter. From the other side however, we have taken into account also inter-dot Coulomb repulsion, while Aono and Eto neglected these correlations [8]. In addition, we have generalized Kotliar-Ruckenstein slave-boson representation by introduction of the slave-bosons not only for single-electron states but also for many-body states: singlet and triplet, formed between electrons resided on different dots. We think that this generalization is crucial to cause aforementioned difference, because important effects of correlations and formation of many-particle states are outside the scope of the usual SBMFA, like e.g. used by Aono and Eto [8].

4 Final remarks

In the paper we presented conductance through serially coupled double quantum dot in presence of inter-dot Coulomb repulsion and ferromagnetic exchange. The

crossover from the atomic to the molecular limit is analyzed in order to show how the conductance in the model depend on the competition between the level broadening and the dot-dot transmission. In the atomic limit we found the double Kondo effect for two electrons, while in the opposite case the conductance vanishes for sufficiently low gate voltages, which means the Kondo effect disappeared. In the molecular limit the conductance and the average occupation of the dot are very sensitive on the influence of the inter-dot Coulomb repulsion and the position of the local energy level. In the case, we have also found the Kondo effect, but for one electron on the DQD. The resonance region is broadened with increasing inter-dot Coulomb repulsion as well as with decreasing exchange interactions.

This work is supported by the Ministry of Science and Higher Education, and the project RTNNANO Contract No. MRTN-CT-2003-504574.

References

1. W.G. van der Wiel et al., Rev. Mod. Phys. **75**, 1 (2003)
2. D.M. Zumbühl, C.M. Marcus, M.P. Hanson, A.C. Gossard, Phys. Rev. Lett. **93**, 256801 (2004)
3. P. Zoller, Th. Beth, D. Binosi, R. Blatt, H. Briegel, D. Bruss, T. Calarco, J.I. Cirac et. al., Eur. Phys. J. D **36**, 203 (2005)
4. G. Burkard, H.A. Engel, D. Loss, Fortschr. Phys. **48**, 965 (2000)
5. W. Izumida, O. Sakai, Phys. Rev. B **62**, 10260 (2000)
6. W. Izumida, O. Sakai, J. Phys. Soc. Jpn **74**, 103 (2005)
7. B.R. Bułka, T. Kostyrko, Phys. Rev. B **70**, 205333 (2004)
8. T. Aono, M. Eto, Phys. Rev. B **63**, 125327 (2001)
9. B. Dong, X.L. Lei, Phys. Rev. B **65**, 241304 (2002)
10. A. Georges, Y. Meir, Phys. Rev. Lett. **82**, 3508 (1999)
11. T. Aono, M. Eto, K. Kawamura, J. Phys. Soc. Jpn **67**, 1860 (1998)
12. R. Aguado, D.C. Langreth, Phys. Rev. Lett. **85**, 1946 (2000)
13. T. Aono, M. Eto, K. Kawamura, Jpn J. Appl. Phys. **38**, 315 (1999)
14. B. Dong, X.L. Lei, Phys. Rev. B **66**, 113310 (2002)
15. B. Dong, H.L. Cui, Semicond. Sci. Technol. **19**, S14 (2004)
16. G. Michałek, B.R. Bułka, Eur. Phys. J. B **28**, 121 (2002)
17. V.M. Apel, M.A. Davidivich, E.V. Anda, C.A. Busser, G. Chiappe, Microelectronics Journal **34**, 729 (2003)
18. P. Coleman, Phys. Rev. B **29**, 3035 (1984)
19. G. Kotliar, A.E. Ruckenstein, Phys. Rev. Lett. **57**, 1362 (1986)
20. P. Coleman, Phys. Rev. B **35**, 5072 (1987)
21. R. Aguado, D.C. Langreth, Phys. Rev. B **67**, 245307 (2003)
22. N. Read, D.M. Newns, J. Phys. C **16**, 3273 (1983)
23. B. Dong, X.L. Lei, J. Phys.: Cond. Matt. **13**, 9245 (2001)
24. B. Dong, X.L. Lei, Phys. Rev. B **63**, 235306 (2001)
25. H. Haug, A.P. Yauho, *Quantum Kinetics in Transport and Optics of Semiconductors* (Springer-Verlag, Berlin, 1998)